Impact of cyclization and methylation on peptide penetration through droplet interface bilayers

Abdou Rachid Thiam, Vincent Faugeras, Olivier Duclos, Didier Bazile, Abdou Thiam

Impact of cyclization and methylation on peptide penetration through droplet interface bilayers

Vincent Faugeras[1,3], Olivier Duclos[2], Didier Bazile[3], Abdou Rachid Thiam[1]*

[1]Laboratoire de Physique de l'École Normale Supérieure, ENS, Université PSL, CNRS, Sorbonne Université, Université de Paris, F-75005 Paris, France

[2]Integrated Drug Discovery Platform. Sanofi R&D, Chilly-Mazarin, France.

[3]Pharmaceutics Development Platform. Sanofi R&D, Gentilly, France,

(*correspondence to thiam@ens.fr)

Abstract

Cell-penetrating peptides enter cells via diverse mechanisms, such as endocytosis, active transport, or direct translocation. For the design of oral-delivered cell-penetrating peptides, it is crucial to know the contribution of these different mechanisms. In particular, the ability of a peptide to translocate through a lipid bilayer remains a key parameter for the delivery of cargos. However, existing approaches used to assess translocation often provide discrepant results, probably because they have different sensitivities to the distinct translocation mechanisms. Here, we focus on the passive permeation of a range of hydrophobic cyclic peptides inspired by somatostatin, a somatotropin release-inhibiting factor. By using droplet interface bilayers (DIB), we assess the passive membrane permeability of these peptides and study the impact of the peptide cyclization and backbone methylation on translocation rates. Cyclization systematically improved the permeability of the tested peptides while methylation did not. By studying the interaction of the peptides with the DIB interfaces, we found membrane insertion and peptide intrinsic diffusion to be two independent factors of permeability. Compared to the industrial gold standard Caco-2 and PAMPA models, DIBs provide intermediate membrane permeability values, closer to Caco-2. Even for conditions where Caco-2 and PAMPA are discrepant, the DIB approach also gives results closer to Caco-2. Thereupon, DIBs represent a robust alternative to the PAMPA approach for predicting the permeability of peptides, even if the latter present extremely small structural differences.

Introduction

Bioavailability represents the yield of a drug that reaches the systemic circulation. It is a crucial parameter for the design of oral drugs. Unfortunately, improvements in drugs specificity and efficiency often come with a loss of intestinal absorption, leading to poor oral bioavailability.[1,2] As such, activity and bioavailability both challenge the development of treatments, especially those for protein-related diseases which require high specificity.[3] By combining the protein-protein blocking capabilities of biologics with the bioavailability of small molecules, some peptides potentially provide a solution to this problem.[4,5]

A growing family of peptides called cell-penetrating peptides (CPP) emerged as a promising family to chaperone active macromolecules through cell membranes, such as oligonucleotides, proteins, and medical imaging agents to target sites.[6] Such an asset makes CCPs potent and versatile candidates for disease treatment.[7,8] However, CPPs often exhibit high proteolytic degradation sensitivity and poor endosomal membrane escape ability.[9,10] Yet, exceptions exist, such as CPPs with constrained patterns, e.g., cycles, staples, or turns.[11] These constraints result in a loss of entropy and the presence of hidden structures in the molecular backbone. Thus, cyclization, for example, likely offers resistance to proteolytic degradations[9], might enhance cell membrane permeability, and, thereupon, represent potent candidates for oral delivery.[12–14] In particular, the constrained structure of hydrophobic cyclic peptides likely offer a higher bilayer membrane permeability.[11,15,16] This is the case of Cyclosporin-A which is a cyclopeptide found in fungi that exhibits a high bioavailability and bioactivity.[17,18] The cyclic nature and multiple backbone N-methylations of Cyclosporin-A has been found to be the key features of its bioavailability.[19,20]

N-methylation can affect conformation and hydrogen bonding potentials. In this way, it may modulate the bioavailability and bioactivity of peptides.[21] Accordingly, multiple pieces of evidence showed a correlation between backbone methylation and membrane permeability.[22–24] Considering structural features that can induce constrained patterns in molecular backbones, somatostatin-inspired peptides were designed to identify minimum sequences required for an efficient cell permeation. Notably, few hexa- and nona-peptides derived from somatostatin showed significant intestinal permeability and oral bioavailability.[13,25]

With the benefits offered by these peptides, several methods have been set up for the early-stage assessment of their activity and bioavailability. They are often based on cell culture methodologies coupled with microscopy studies.[26,27] Unfortunately, such methods are not suitable for the pharmaceutical industry because of frequent reproducibility issues and inability to scale them up to high throughput screening. Therefore, most permeability studies

rely on Caco-2 cell models and PAMPA systems. Caco-2 cells are small intestine cells put in culture to mimic the intestinal barrier. This method cumulates contributions from both passive and active permeabilities, and diffusion through cell junctions, which cannot be decorrelated. PAMPA is based on a filter plate made of pores, infused with a micrometer thick solution of phospholipids in oil, and placed between two aqueous compartments.[28–31] Despite the presence of phospholipids, the water-oil-water film is distinct from phospholipid bilayer membranes.

Model membranes are a suitable tool to assess the passive membrane permeability of peptides, potentially translatable to on-chip high throughput systems. Unilamellar vesicles particularly enable to assess the ability of polycationic and amphipathic peptides to cross cell membranes and to depict permeation mechanisms.[32–35] Droplet interface bilayers (DIBs) are droplet-based method which represent an interesting alternative for identifying peptides-cargo systems suitable for membrane transport.[36–38] Indeed, DIBs are versatile, made rapidly with controlled membrane composition, and they offer a straightforward visualisation and quantification of permeation.[39–42]

Here, we used DIBs to study the passive permeation of a range of hydrophobic peptides derived from somatostatin, a somatotropin release-inhibiting factor. The impact of cyclization and backbone methylation on the resulted permeability was studied. Cyclization improved the permeation of the tested peptides. Methylation also improved permeation but not systematically. By exploring the physical chemistry of the interaction of the peptides with the DIB bilayer, we discussed possible hypotheses for the increased permeability of the peptides.

Results and discussion

Droplet pairing and permeability determination. With a millifluidic device, we generated separately donor (filled with peptides) and acceptor water droplets in an oil phase containing phospholipids. Binary droplets decorated with a monolayer of phospholipids were then brought together under the microscope (**Figure 1.a**). When the droplets were approached to each other, they spontaneously adhered and formed a droplet interface bilayer (DIB).[38,43] The bilayer was fully formed within a minute, depending on the solvent and phospholipids used.[44] We used glyceryl trioctanoate (TO) for the oil phase and DOPE for phospholipids unless stated otherwise. We previously showed that the passive permeability of soluble fluorophores to such a DIB bilayer is similar to that of common membranes.[41,45]
We used a buffer solution containing 50 mM HEPES, 120 mM KAcetate, and 1 mM $MgCl_2$ in Milli-Q water (pH 7.4, 293 mOsm, I = 173 mM) with an addition of DMSO (5 % v/v), enabling a complete dissolution of the peptides at the concentration of 5 µM, used for all experiments. The buffer osmolarity of ~ 300 mOsm was slightly reduced by the addition of DMSO but maintained in a physiological range. Peptides at 5 µM barely modulated the buffer osmolarity. Thus, osmotic fluxes between donor and acceptor compartments are nonexistent.

For the studied peptides, the possible partitioning to the oil phase was largely negligible in front of their membrane permeation rate. The concentration of the fluorescent peptide in the acceptor droplet was thus obtained from the following mass conservation: $C_a V_a + C_d V_d = C_{d0} V_d$ where C is the concentration and V is the volume; "a" denoting for acceptor and "d" for donor compartment; C_{d0} is the concentration of the solute in the donor droplet at t_0. Since the concentration is proportional to the fluorescence intensity F, $C_a \,/\, C_d = F_a \,/\, F_d$ the mass conservation can be written simply as: $C_a V_a + C_a(\frac{F_d}{F_a}) V_d = C_{d0} V_d$

which yields:

$$\frac{C_a}{C_{d0}} = \frac{V_d}{V_a + \frac{V_d \,.\, F_d}{F_a}}$$

Here, the contribution of bleaching is irrelevant since we consider the ratio of the fluorescence between the acceptor and donor droplets that would be similarly bleached. We defined the translocation parameter at 30 minutes p_{30} as:

$$p_{30} = \frac{C_{a30} - C_{a0}}{C_{d0}} \frac{V_a}{A.\Delta t}$$

which quantifies the permeability of the bilayer to the considered analyte (**Figure 1.b**). During permeation, the volume of the droplets V and the patch area A were almost constant (**Figure**

S1.a). Unless mentioned otherwise, the fluorescent probe used to study the peptides' translocation and distribution was the fluorescein-derivative TAMRA, attached to the lysine residue of the peptide (**Figure S2.a,b**).

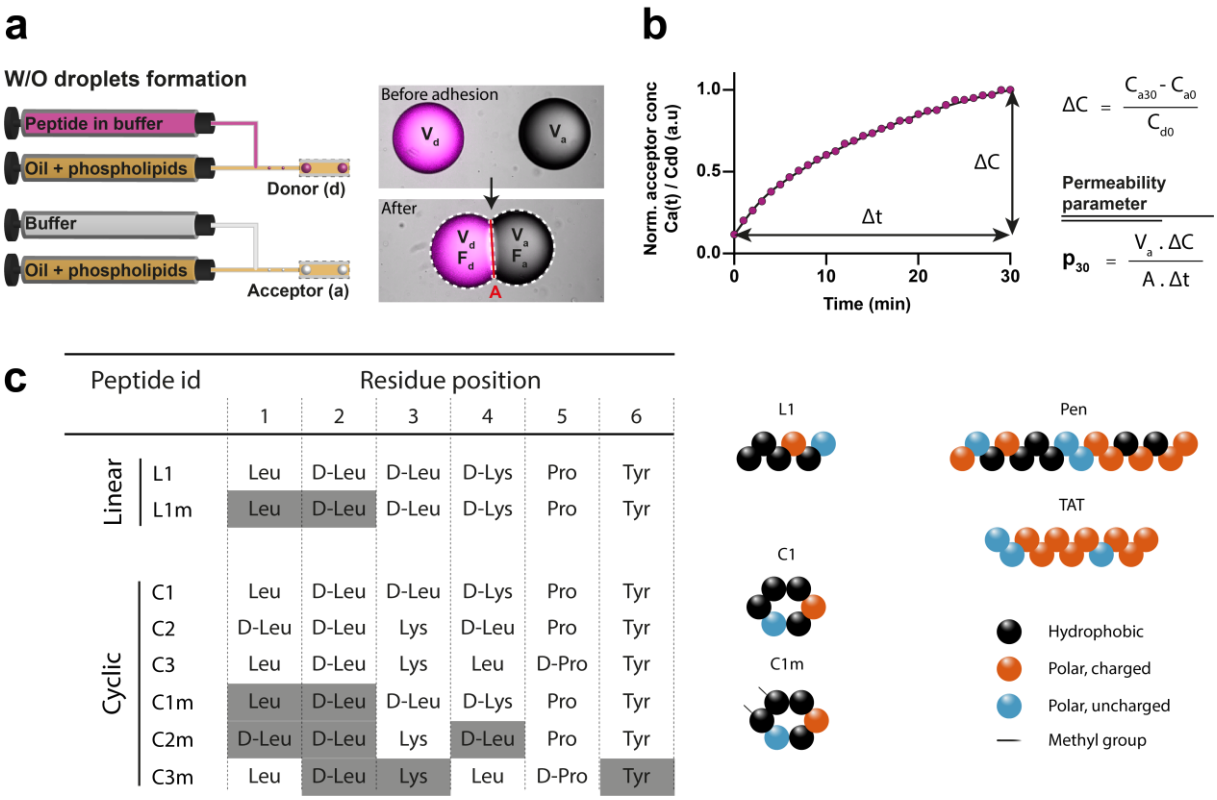

Figure 1: Passive permeability DIB assay with hydrophobic peptides. a) Left: Schematic of the proposed DIB permeability assay. Two sets of W/O droplets, empty and peptide-filled (respectively acceptor and donor droplets), are produced with a millifluidic device and dropped on a treated glass slide for monitoring under a confocal microscope. Right: Microscopic pictures showing droplet paring and DIB parameters. Scale bars, 100 µm. b) Example of permeation kinetics of peptide L1 through glyceryl trioctanoate DOPE DIB; introduction of permeation parameter p_{30}. c) Sequence of the studied peptides, specific methylations are highlighted in grey.

Cyclization significantly increases permeation rate. We investigated the impact of cyclization for a range of peptides derived from somatostatin (**Figure 1.c; L** stands for linear, **C** for cyclic, m for methylated). **C1**, the cyclic counterpart of L1 was found to be much more permeable (**Figure 2.a-c**). Indeed, permeability was improved by about one order of magnitude by cyclization, from $1.4.10^{-7}$ cm.s^{-1} to $1,0.10^{-6}$ cm.s^{-1}. Yet, both peptides have similar chemical properties (MW, hydrophilicity). Importantly, we attached a specific terminal group, acetamide for both N- and C- terminus, to prevent their ionization (**Figure S2.a**). Thus, the net charges of peptides **L1** and **C1** were equal and the difference in permeation should then result from the cyclization of the peptide.

We also compared the cyclic peptide **C1** with well-established linear peptides, the polycationic **TAT,** and the amphipathic Penetratin (**Pen**). Likewise, the linear peptides were much less permeable compared with the cyclic **C1,** with respectively $5.3.10^{-8}$ cm.s^{-1} for **Pen**, $1.4.10^{-8}$ cm.s^{-1} for **TAT,** and $1.8.10^{-7}$ cm.s^{-1} for **C1 (Figure S3.a-d)**. Yet, these discrepancies may not be solely ascribed to the cyclic nature of C1, as the peptides have different net charges, 0, 8, and 9 respectively for **C1**, **Pen,** and **TAT**. Indeed, charge is a determinant parameter for leaving the water environment and to cross the bilayer.

Our findings are consistent with several studies showing that cyclic peptides are better permeants than their linear counterparts.[46,47] However, whether cyclization systematically improves permeability may depend on the amino acid sequence.[48] In any case, designing peptides to increase their lipophilicity and reduce interaction with solvents will improve their permeation.[49] The contribution of cyclization in this picture is likely related to constraints in the molecular structure of the peptide, e.g., through hiding H-bond in the backbone and exposing hydrophobic group.[28] Indeed, such constraint would increase the apparent lipophilicity, reduce interactions with the solvent and, hence, improve permeation rates.

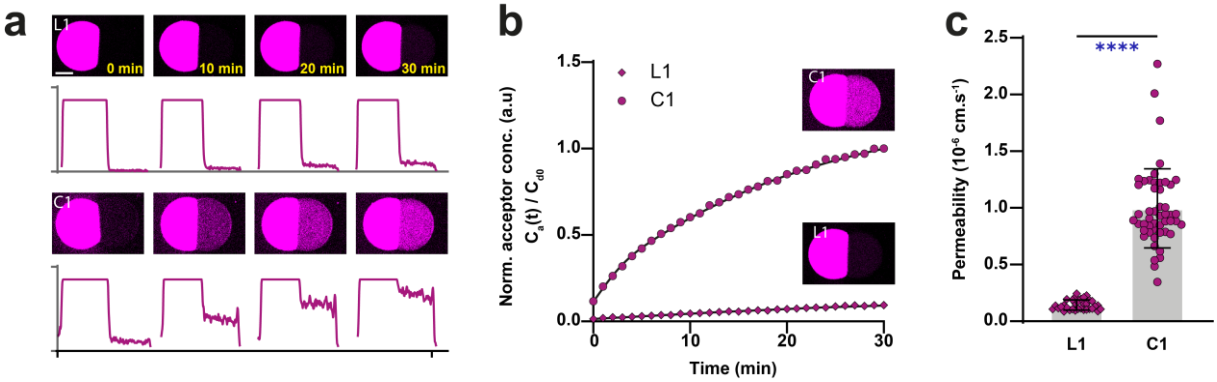

Figure 2: Comparison of the linear and cyclic peptides L1 and C1. a) Confocal microscopy pictures of DIB permeation assay for L1 and C1 peptides over time. The same signal enhancement correction was applied to every single image to be able to detect significative signals of translocation for both peptides (image brightness is enhanced). Corresponding L1 and C1 fluorescence profiles are provided. Scale bars, 100 µm. b) Permeation kinetics for peptides L1 and C1. c) Calculated permeability for L1 and C1 peptides (defined as permeation parameter p_{30}) (mean value, error bars represent the SD; **** indicates $p < 0.0001$).

Impact of backbone N-methylation on permeation. We investigated the impact of amide group methylations on permeation rate for the same group of peptides. To do so, we designed a methylated counterpart of **C1** peptide, **C1m (Figure 1.c)**, with two methylated amide groups on its two first leucine residues. Compared to **C1**, **C1m** showed a significant

increase in permeation **(Figure 3.a-b)**. Permeability increased from $1.0.10^{-6}$ $cm.s^{-1}$ for **C1** to $3.7.10^{-6}$ $cm.s^{-1}$ for **C1m**.

We decided to change the nature of the cargo dye, by using a FITC-labelled analog, to test whether our findings hold (**Figure S3.b,c; (f) stands for FITC-labelled**). The impact of methylation on permeability for **C1** was then studied by repeating the permeation assay. First, we found the permeation rate to differ from TAMRA. Indeed, for the FITC cargo, we measured reduced permeability values, from $1.0.10^{-6}$ $cm.s^{-1}$ to $1,77.10^{-7}$ $cm.s^{-1}$ and $3.7.10^{-6}$ $cm.s^{-1}$ to $1,43.10^{-6}$ $cm.s^{-1}$, respectively for **C1(f)** and **C1m(f)**. These variations indicated that the nature of the cargo modulated permeability. Here, the slowdown in permeation may be ascribed to the net charge difference between FITC, having two additional charges, and the zwitterionic TAMRA at our physiological-working pH. Second and foremost, **C1m(f)** still had a much higher permeability than **C1(f)**, by almost an order of magnitude (**Figure S3.b, c**). Thus, we found that methylation improved the permeability of the cyclic peptide **C1** with two different cargos.

We also studied whether methylation improves the permeability of the corresponding linear **L1**. Like **C1m**, **L1m** features two methylated groups on the same residues (two first leucine residues). As between **L1** and **C1**, **L1m** had a lower permeation rate than **C1m**, i.e. $3.1.10^{-8}$ $cm.s^{-1}$ to $3.7.10^{-6}$ $cm.s^{-1}$, a two orders magnitude difference **(Figure 3.c)**. While **C1m** had a higher permeability than **C1**, it is interesting to note that the permeability for **L1m** was significantly reduced compared to **L1**. This trend could be due to the reduction of donor H-bond for methylated **L1m**, which would reduce the possibilities of intramolecular H-bonding constraining the peptide. In any case, these findings support that the relevance of methylation in improving permeability is likely more prominent to cyclic peptides.

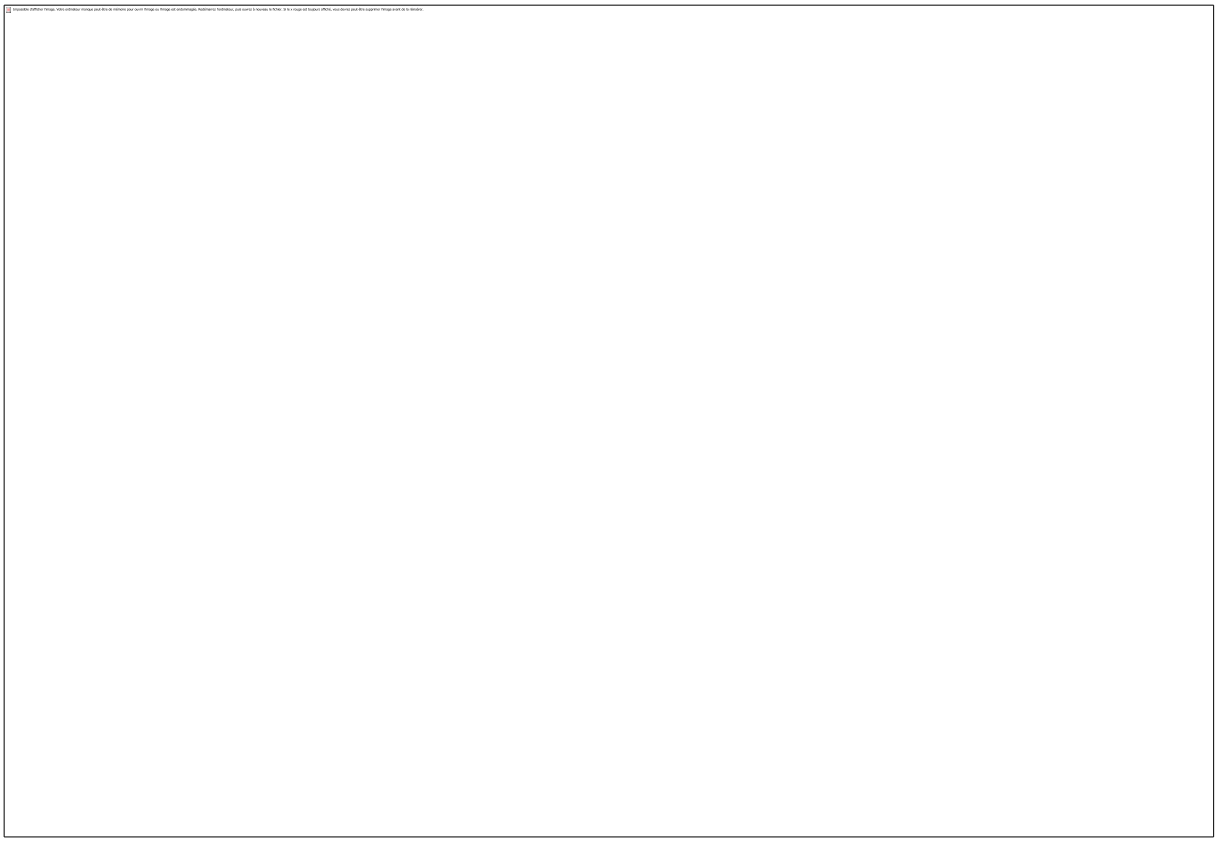

Figure 3: Comparison of cyclic peptides C1 and C1m. a) Confocal microscopy pictures of DIB permeation assay for C1 and C1m peptides over time. Corresponding C1 and C1m fluorescence profiles are provided. Scale bars, 100 µm. b) c) Calculated permeability for C1, C1m, L1 and L1m peptides (defined as permeation parameter p_{30}) (mean value, error bars represent the SD; **** indicates $p < 0.0001$).

Methylation does not systematically improve the permeation rate of cyclic peptides. To further study the impact of methylation on permeation, we considered two new cyclic peptides, **C2** and **C3 (Figure 1.c)**. These peptides have the same amino acids sequence as **C1,** except that the lysine residue was switched to the neighbor leucine residue at position 3 for labeling purposes (**Figure 1.c**). The difference between these peptides mostly lies in the position and the number of D amino acids, known to modulate molecular conformations (**Figure 1.c**).[50] **C2m** and **C3m** are respectively the methylated counterpart of **C2** and **C3** with three specific methylations, when **C1m** possesses two methylations at different amino acids (**Figure 1.c**).

Despite their similar amino acid content, **C1**, **C2**, and **C3** had very different permeabilities (**Figure 4.a, b**). For instance, **C1** had a lower permeability compared to **C2**, or **C3**. This result indicates that the amino acid chirality is crucial, probably through altering intramolecular

interactions constraining the cycle. Regarding the impact of methylation for **C2** and **C3**, we obtained different behaviors. Permeability was decreased by methylation between **C2** and **C2m**, i.e., from $5.6.10^{-6}$ cm.s^{-1} and $2.4.10^{-6}$ cm.s^{-1}, but increased by methylation between **C3** and **C3m**, $2.6.10^{-6}$ cm.s^{-1} and $3.7.10^{-6}$ cm.s^{-1} (**Figure 4.b**). Thus, for **C1** and **C3**, and not **C2**, methylation improved permeability.

Methylation may modulate both peptide lipophilicity and interaction with the solvent. When amides are methylated, peptide interaction with the solvent is decreased through the reduction of H-bonds. In this way, methylation might confer higher intramolecular constraints.[28] These constraints may reduce conformational possibilities offering interactions with water molecules and, thereupon, improve permeability. This might have been the case for **C1m** and **C3m**. Yet, the position of the methylation would be crucial as it could also prevent intramolecular H-bonding. In such an eventuality, the nature of the resulting constraint may not be favorable for membrane permeation. This might have occurred with **C2m** that showed reduced permeability compared to **C2**. In conclusion, the methylation of cyclic peptides can improve the passive permeability but not systematically, and the methylation position might be detrimental to the improvement of permeability.

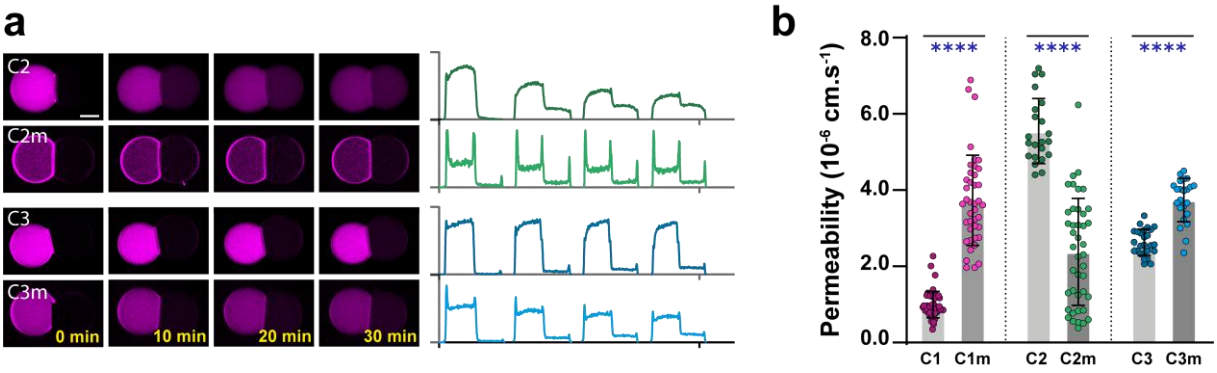

Figure 4: Comparison of cyclic peptides C1, C1m, C2, C2m, C3, and C3m. a) Confocal microscopy pictures of DIB permeation assay for C2, C2m, C3, and C3m peptides over time. Corresponding fluorescence profiles are provided. Scale bars, 100 µm. b) Calculated permeability for C1, C1m, C2, C2m, C3 and C3m peptides (defined as permeation parameter p_{30}) (mean value, error bars represent the SD; **** indicates $p < 0.0001$).

The DIB assay represents an accurate model for permeability assessment. The permeability of the studied peptides was assayed with the industrial gold-standard methods PAMPA and Caco-2 (**Figure 5.a**).[49] However, the results with these methods are often discrepant.[28] In the PAMPA approach, a phospholipid bilayer is not generated and does not reproduce properly a phospholipid bilayer. The Caco-2 approach cumulates multiple permeabilities: through cell junctions, passive permeability across the plasma membrane,

and permeability via endocytic pathways. Thus, it may not be surprising that these methods become discrepant for specific conditions. Also, these methods would not yield the absolute bilayer permeability, as model bilayers such as DIBs would enable. Therefore, we decided to compare the permeability values of the cyclic peptides between the three approaches.

The permeability values of **C1**, **C1m**, **C2**, **C2m**, **C3**, and **C3m** were evaluated via PAMPA and Caco-2 cells by Wang et al. (2015).[49] Considering the impact of the fluorescent cargo reporter we attached to the peptides, we renormalized all results and analyzed the relative permeability of the peptides for each assay (**Figure 5.b**). Overall, we found that permeability values from the DIB assay were intermediate between PAMPA and Caco-2 assays. Yet, while the permeability value for **C3m** relative to **C3** shows a decrease of permeability in the case of PAMPA (0.5 times), it is increased for the DIB (1.4 times) and Caco-2 (13 times) assays. Moreover, methylated peptides showed close permeability patterns for the DIB and Caco-2 assays when PAMPA significantly underestimates the value for **C2m** and **C3m** relative to **C1m** (**Figure 5.b**). These comparisons reveal that the DIB assay is an encouraging approach to evaluate the passive permeability of peptides, given that Caco-2 and PAMPA might misevaluate permeability. This will be especially the case when peptides can cross cell membranes through several mechanisms. In such a case, Caco-2 might overestimate the passive permeability, e.g., because of active transports or para- and trans-cellular diffusion, while PAMPA might underestimate the permeation efficiency because of the thick layer of oil between the two phospholipid monolayers. Collectively, our results suggest that the DIB assay reflects better than PAMPA the passive permeability of peptides across bilayers and it is a good compromise between PAMPA and Caco-2.

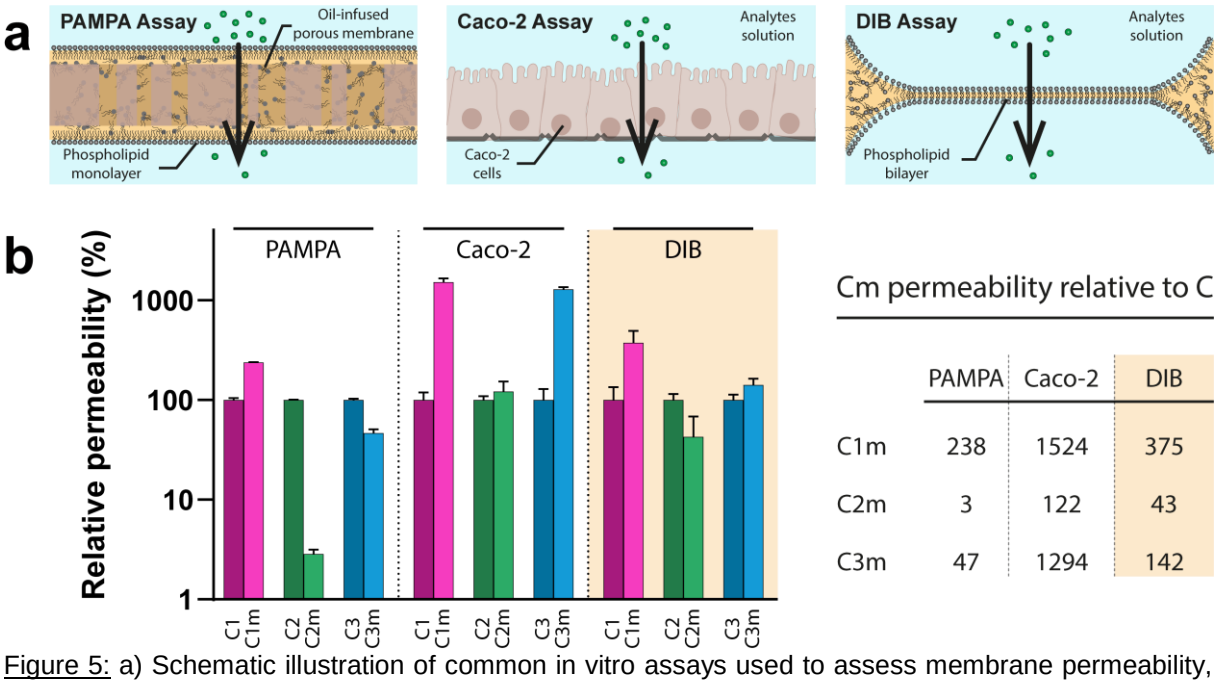

Cm permeability relative to C

	PAMPA	Caco-2	DIB
C1m	238	1524	375
C2m	3	122	43
C3m	47	1294	142

Figure 5: a) Schematic illustration of common in vitro assays used to assess membrane permeability,

PAMPA wells, Caco-2 cells, and DIBs assays. b) Relative permeability value measured via PAMPA and Caco-2 assays (renormalized from Wang et al., 2015), and the proposed DIB assay. Methylated peptide permeability values are defined as a percentage of the corresponding unmethylated peptide permeability value.

Permeability dependence on membrane recruitment. We found that the peptides were recruited to the DIB interfaces (**Figure 3.a, 4.a**). Since their translocation requires contact with the membrane, we asked whether the interfacial signal of the peptides could be a proxy for permeability.

We defined an interfacial recruitment parameter, R_m and R_b, respectively quantifying the signal of the peptides on the monolayer and the bilayer (**Figure 6.a**). Methylation systematically increased the interfacial recruitment R_m and R_b of the cyclic peptides (**Figure 6.b,c**). To know whether the peptides were inserted between phospholipids, we conducted the assay with a lipid composition offering a better tightening of the phospholipid bilayer.[41,51] Namely, we used a phospholipid composition made of DOPE:DOPC 1:1. With this new composition, the peptides were almost totally excluded from the interface (**Figure S4.a,b**). Therefore, the phospholipid bilayer packing level correlates with the capacity of the peptides to insert into the membrane. Methylated peptides have thus a higher tendency to insert. Interestingly, the decrease in the peptide recruitment level to the bilayer was accompanied by a reduction in permeability for **C1m**, from $3.7.10^{-6}$ $cm.s^{-1}$ for DOPE and $1.5.10^{-6}$ $cm.s^{-1}$ for DOPE:DOPC 1:1 (**Figure S4.b**). At least for this peptide, the insertion capacity of the peptides seems to correlate with permeability.

To further verify our conclusion, we plotted all the permeability values for each peptide as a function of the bilayer recruitment $R_{b,}$ and regardless of the membrane composition. We observed that permeability tends to increase with R_b for both **C1/C1m** and **C3/C3m** pairs (**Figure 6.d**); we noticed an almost linear dependence between the peptide recruitment to the phospholipid bilayer with permeability (**Figure 6.d**). For these peptides, the recruitment to the bilayer seemed determinant to permeation. Their membrane recruitment was likely mediated by the hydrophobic residues in the peptides (L, Y) [52,53] and the methylation at the Leucine could improve their orientation and interaction with the membrane. For instance, such a membrane recruitment-based mechanism promotes the translocation of amphipathic peptides.[15,54]

However, **C2/C2m** showed inconsistent behaviors (**Figure 6.d**), as its translocation rate was not reflected by its interfacial recruitment (except if **C2m** was considered alone). This observation indicates that the capacity of a peptide to insert into the bilayer membrane

represents only one parameter controlling permeability. Other parameters might become more prominent depending on the nature of the peptide, as for **C2**. Thus, although the peptide insertion in the bilayer could be a proxy for permeability, the insertion level does not systematically correlate with the penetrating ability of the peptide. This will be especially true for peptides having a high intrinsic translocation capacity, e.g., with high flexibility allowing them to fit both hydrophilic and hydrophobic environment.

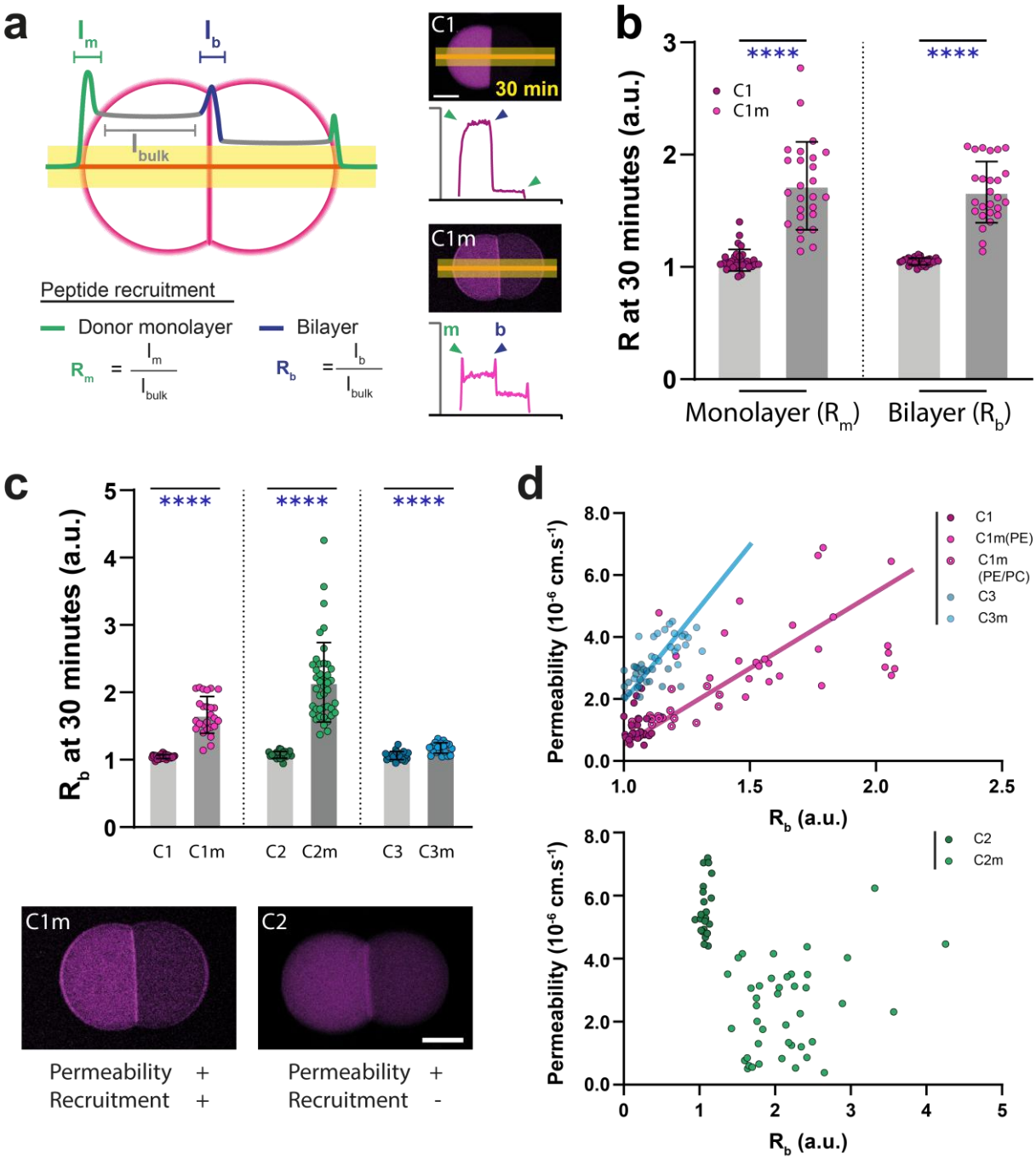

Figure 6: a) Schematic representation of DIB and the associated method to obtain fluorescence profile and peptide recruitment R_m and R_b. Scale bars, 100 µm. b) Monolayer donor (mD) and bilayer (b) recruitment values for peptides C1 and C1m. c) Bilayer recruitment values R_b for all three peptide couples (C1, C1m, C2, C2m, C3, C3m) d) Permeability value for each DIB assays as a function of

peptide recruitment on the bilayer R_b. Top: for C1 and C3 couples, Bottom: for C2 couple. (mean value, error bars represent the SD; **** indicates $p < 0.0001$).

Conclusion

Poor intestinal permeability is a key limitation to the development of bioavailable drugs suitable for oral delivery. Therefore, there is a crucial need for assays that can enable robust and high-throughput measurement of cell permeability. Current gold-standard systems are PAMPA wells and Caco-2 cells.[55] However, the permeability of many compounds assessed with these systems was discrepant.[56] In this study, we used a biomimetic DIB assay to investigate the permeability of various molecules tested by these methods and highlight determinant features that had not been revealed. We found that DIB assay can efficiently discriminate peptides based on their structure when they have similar amino acid content. Indeed, tiny structural modifications such as amide methylation or amino acids chirality inversion induced significant changes in peptide permeation through bilayers. The DIB assays allowed us to quantify permeability variations in three orders of magnitude, with intermediate performance between PAMPA and Caco-2. Altogether, the DIB assay appears as a solid alternative to PAMPA to study cell permeability and is highly complementary to Caco-2. It demonstrates the ability to consistently distinguish the passive permeation capacity of peptides designed with tiny structural differences. Translating this assay into high throughput will make it a promising tool for the pharmaceutical industry.

Material and Method

Products. All phospholipids (Avanti Polar Lipids), glyceryl trioctanoate (Sigma-Aldrich), fluorescein sodium salt (VWR Chemicals), HEPES (Sigma-Aldrich), potassium acetate KCH_3COO (Sigma-Aldrich) and magnesium chloride $MgCl_2$ (Sigma-Aldrich) are used without further purification. Penetratin and TAT peptides were purchased at Anaspec. Linear peptides L1, L1m and cyclic peptides C2, C2m, C3, C3m were synthesized at Peptides & Elephants GmbH. Other cyclic peptides were purchased by Peptides International (USA). Structure and purity were respectively checked by mass spectroscopy and HPLC (purity > 90 %).

Unless mentioned otherwise, peptides are first aliquoted down to 100 µM in a mixture of HKM buffer and DMSO (50/50% v/v) suitable for the complete dissolution of peptide. Peptide samples are then diluted down to 5 µM for W/O droplets fabrication and assays.

Preparation of the Oil Phase. Phospholipids used for the oil phase are conditioned in chloroform. We first evaporate chloroform under a stream of argon; the dried lipids are subsequently re-solubilized to the desired concentration in glyceryl trioctanoate (TO). Unless stated otherwise, a lipid concentration of 0.1 wt% is used for all experiments, this value is above the critical concentration for every studied phospholipid composition.

Millifluidic setup to fabricate monodisperse W/O droplets. Experiments are performed with a 0.1 wt. % lipids in TO solution and the following HKM buffer recipe: 50 mM HEPES, 120 mM KCH_3COO, and 1 mM $MgCl_2$ in Milli-Q water (at pH 7.4). For our assays, it is necessary to produce two types of droplets: acceptor droplets filled with buffer and donor droplets filled with a 5 µM solution of peptides in buffer. To do so, we use two parallel circuits composed of two Nemesys syringe pumps (Cetoni GmbH, Deutschland) enabling the injection of the oil continuous phase and the aqueous dispersed phase. The tubes (250 µm ID, 1,6 mm OD) coming from 1000 µL dispensing syringes (Gastight 1000 µL, Hamilton Company, US) are connected via a T-junction (IDEX Health & Science LLC, US) that enables the formation of W/O droplets. Flow rates for the oil and aqueous solution are respectively fixed at Q_O = 1000 µL.h^{-1} and Q_W = 200 µL.h^{-1} resulting in about 280 ± 10 µm diameter droplets. We finally placed the generated two families of droplets on a glass slide coated with PDMS and treated with the water repellent Rain-X (ITW Global Brands, US), it allows to prevent droplets from wetting the substrate and collapsing (**Figure 1.b**).

Permeability Assay. All permeability assays are conducted at room temperature T_{lab} = 21°C under a laser scanning microscope (LSM 800, Carl Zeiss, Oberkochen, Germany). Two droplets, one acceptor and one donor are selected. We then bring the droplets into contact enabling the adhesion of monolayers and the spontaneous formation of a bilayer. Just after DIB formation, we follow the passage of the analyte through the interface by taking pictures of the droplets every minute. The permeation is studied over 30 minutes (**Figure 1.a,b**).

Quantification of permeability. The analyte concentration is proportional to the fluorescence intensity. The initial concentration in the acceptor droplet is considered negligible, giving $C_{a0} = 0$ mol.L^{-1}, even though a little fraction of solute can diffuse through the oil or translocate through the bilayer during the monolayer adhesion process. Mass conservation equation is given by:

$$C_a V_a + C_d V_d = C_{d0} V_d$$

where $V_{a\ or\ d}$ and $C_{a\ or\ d}$ are respectively the volume and concentration of the acceptor and donor droplets; C_{d0} is the initial concentration of the donor droplet. We consider that the volume and the patch area do not vary throughout the permeation process (**Figure S1.a**).

We use the confocal images of DIBs to measure the concentration of fluorescein in donor and acceptor droplets. As fluorescence intensity is proportional to concentration, we are able to study the evolution of the acceptor and donor concentration (**Figure S5**). Note that we kept the same laser parameters from one experiment to one another. The concentration in the acceptor droplet is obtained following mass conservation equation:

knowing that $C_a = sF_a$ and $C_d = sF_d$, where $F_{\mathrm{a,d}}$ denotes the respective fluorescence intensity in donor and acceptor droplets and s the proportionality factor, one can write:

$$C_a V_a + C_a \left(\frac{F_d}{F_a}\right) V_d = C_{d0} V_d$$

which yields

$$\frac{C_a}{C_{d0}} = \frac{V_d}{V_a + \frac{V_d \,.\, F_d}{F_a}}$$

Note that F_d / F_a annihilates the bleaching effect. By measuring the droplets' volume and intensity, the value of C_a / C_{d0} is known. To be able to properly measure concentration in acceptor droplet for peptides of low permeation rate, we subtracted noise signal to fluorescence from droplets (**Figure S5**):

$$\frac{C_a}{C_{d0}} = \frac{V_d}{V_a + \frac{V_d \,.\, (F_d - F_{\mathrm{n}})}{(F_a - F_{\mathrm{n}})}}$$

We finally define the translocation parameter at 30 minutes: p_{30} as:

$$p_{30} = \frac{C_{a30} - C_{a0}}{C_{d0}} \frac{V_a}{A.\Delta t}$$

Where C_{a30} and C_{a0} are respectively the measured peptide concentration at t = 30 min and the initial peptide concentration in the acceptor droplet, A is the patch area and Δt is the duration of the experiment (here 30 minutes). The translocation ratio is weighted with both V_a and A to consider variation in droplet morphology and divided by Δt_{30} to be homogeneous to a permeability. Each permeability value was determined by its mean and standard deviation. We performed a minimum of 10 measurements for each peptide or lipid composition. The quantification process from the raw data is summarized in **figure S5.**

Morphological analysis of DIBs. Compartment volumes $V_{a\,or\,d}$ are measured from a brightfield picture taken before droplet adhesion. Contact area A is obtained from the mean value of patch radius measured throughout the experiment. We also measure the contact angle robustly from droplets and patch radii with the following equation:

$$2\theta = sin^{-1}\left(\frac{R_p}{R_a}\right) + sin^{-1}\left(\frac{R_p}{R_d}\right)$$

where R_p and $R_{a\,or\,d}$ are respectively the radii of patch, acceptor and donor droplets during adhesion. As an example, see **figure S1.a**.

Measurement of monolayer and bilayer peptide recruitment. From confocal microscopy picture of DIBs, we can study the interfacial behaviour of peptides. The fluorescent intensity profile is obtained via mean segment profile integration (25 px lateral integration) for each droplet interface bilayers (**Fig. 6a**). We then introduce a peptide recruitment factor calculated from the mean fluorescence value of droplet bulk and the

maximum fluorescence intensity on bilayer and/or monolayers. The peptide recruitment factor is defined as:

$$R_m = \frac{\max(m_{d/a})}{\text{mean}(bulk_{d/a})} \quad and \quad R_b = \frac{\max(b)}{\text{mean}(bulk_d)}$$

Where b, $bulk_{d/a}$ and $m_{d/a}$ respectivly refer to the bilayer, the bulk and the monolayer of donor/acceptor droplet fluorescence intensity (a.u.). Peptide recruitment was considered at the end of the permeability assay, after 30 minutes, letting enough time for peptide to reach interfacial equilibrium.

Quantification and statistical analysis. Statistical significance was evaluated by Welch's t tests (unpaired parametric test, two-tailed P value) using Prism 8.0 (GraphPad Software, US). All values shown in the text and figures are mean ± S.D, and taken from at least 3 experiments (ns indicates $p > 0.05$ not significant, * indicates $p < 0.05$, ** indicates $p < 0.01$, *** indicates $p < 0.001$, **** indicates $p < 0.0001$).

Supporting information

Peptide details and additional data (control experiments, FITC-labeled peptides permeation behavior, data treatment) are provided.

References

(1) Macarron, R.; Banks, M. N.; Bojanic, D.; Burns, D. J.; Cirovic, D. A.; Garyantes, T.; Green, D. V. S.; Hertzberg, R. P.; Janzen, W. P.; Paslay, J. W.; Schopfer, U.; Sittampalam, G. S. Impact of High-Throughput Screening in Biomedical Research. *Nat. Rev. Drug Discov. 2011 103* **2011**, *10* (3), 188–195. https://doi.org/10.1038/nrd3368.

(2) Gard, P. R. *Applied Pharmacology*; Elsevier/Saunders, 2020. https://doi.org/10.1201/9781482267976-15.

(3) Kola, I.; Landis, J. Can the Pharmaceutical Industry Reduce Attrition Rates? *Nat. Rev. Drug Discov.* **2004**, *3* (8), 711–715. https://doi.org/10.1038/nrd1470.

(4) Morrison, C. Constrained Peptides' Time to Shine? *Nat. Rev. Drug Discov.* **2018**, *17* (8), 531–533. https://doi.org/10.1038/nrd.2018.125.

(5) Martin-Loeches, I.; Dale, G. E.; Torres, A. Murepavadin: A New Antibiotic Class in the Pipeline. *Expert Rev. Anti. Infect. Ther.* **2018**, *16* (4), 259–268. https://doi.org/10.1080/14787210.2018.1441024.

(6) Patel, L. N.; Zaro, J. L.; Shen, W. C. Cell Penetrating Peptides: Intracellular Pathways and Pharmaceutical Perspectives. *Pharm. Res.* **2007**, *24* (11), 1977–1992. https://doi.org/10.1007/s11095-007-9303-7.

(7) Chugh, A.; Eudes, F.; Shim, Y. S. Cell-Penetrating Peptides: Nanocarrier for Macromolecule Delivery in Living Cells. *IUBMB Life* **2010**, *62* (3), 183–193. https://doi.org/10.1002/iub.297.

(8) Zhang, P.; Monteiro da Silva, G.; Deatherage, C.; Burd, C.; DiMaio, D. Cell-Penetrating Peptide Mediates Intracellular Membrane Passage of Human Papillomavirus L2 Protein to Trigger Retrograde Trafficking. *Cell* **2018**, *174* (6), 1465-1476.e13. https://doi.org/10.1016/j.cell.2018.07.031.

(9) Shibata, K.; Suzawa, T.; Soga, S.; Mizukami, T.; Yamada, K.; Hanai, N.; Yamasaki, M. Improvement of Biological Activity and Proteolytic Stability of Peptides by Coupling with a Cyclic Peptide. *Bioorganic Med. Chem. Lett.* **2003**, *13* (15), 2583–2586. https://doi.org/10.1016/S0960-894X(03)00476-1.

(10) Verdurmen, W. P. R. R.; Mazlami, M.; Plückthun, A. A Quantitative Comparison of Cytosolic Delivery via Different Protein Uptake Systems. *Sci. Rep.* **2017**, *7* (1), 1–13. https://doi.org/10.1038/s41598-017-13469-y.

(11) Qian, Z.; Martyna, A.; Hard, R. L.; Wang, J.; Appiah-Kubi, G.; Coss, C.; Phelps, M. A.; Rossman, J. S.; Pei, D. Discovery and Mechanism of Highly Efficient Cyclic Cell-Penetrating Peptides. *Biochemistry* **2016**, *55* (18), 2601–2612. https://doi.org/10.1021/acs.biochem.6b00226.

(12) Gentilucci, L.; De Marco, R.; Cerisoli, L. Chemical Modifications Designed to Improve Peptide Stability: Incorporation of Non-Natural Amino Acids, Pseudo-Peptide Bonds, and Cyclization. *Curr. Pharm. Des.* **2010**, *16* (28), 3185–3203. https://doi.org/10.2174/138161210793292555.

(13) Liu, T.; Liu, Y.; Kao, H. Y.; Pei, D. Membrane Permeable Cyclic Peptidyl Inhibitors against Human Peptidylprolyl Isomer Ase Pin1. *J. Med. Chem.* **2010**, *53* (6), 2494–2501. https://doi.org/10.1021/jm901778v.

(14) Bock, J. E.; Gavenonis, J.; Kritzer, J. A. Getting in Shape: Controlling Peptide Bioactivity and Bioavailability Using Conformational Constraints. *ACS Chem. Biol.* **2013**, *8* (3), 488–499. https://doi.org/10.1021/cb300515u.

(15) Jobin, M. L.; Blanchet, M.; Henry, S.; Chaignepain, S.; Manigand, C.; Castano, S.; Lecomte, S.; Burlina, F.; Sagan, S.; Alves, I. D. The Role of Tryptophans on the Cellular Uptake and Membrane Interaction of Arginine-Rich Cell Penetrating Peptides. *Biochim. Biophys. Acta - Biomembr.* **2015**, *1848* (2), 593–602. https://doi.org/10.1016/j.bbamem.2014.11.013.

(16) Hoang, H. N.; Hill, T. A.; Fairlie, D. P. Connecting Hydrophobic Surfaces in Cyclic Peptides Increases Membrane Permeability. *Angew. Chemie* **2021**, *133* (15), 8466–8471. https://doi.org/10.1002/ANGE.202012643.

(17) Tjia, J.; Webber, I.; Back, D. Cyclosporin Metabolism by the Gastrointestinal Mucosa. *Br. J. Clin. Pharmacol.* **1991**, *31* (3), 344–346. https://doi.org/10.1111/j.1365-2125.1991.tb05540.x.

(18) Borel, J. F.; Feurer, C.; Gubler, H. U.; Stähelin, H. Biological Effects of Cyclosporin A: A New Antilymphocytic Agent. *Agents Actions* **1976**, *6* (4), 468–475. https://doi.org/10.1007/BF01973261.

(19) Räder, A. F. B.; Reichart, F.; Weinmüller, M.; Kessler, H. Improving Oral Bioavailability of Cyclic Peptides by N-Methylation. *Bioorganic Med. Chem.* **2018**, *26* (10), 2766–2773. https://doi.org/10.1016/j.bmc.2017.08.031.

(20) Hill, T. A.; Shepherd, N. E.; Diness, F.; Fairlie, D. P. Constraining Cyclic Peptides to Mimic Protein Structure Motifs. *Angew. Chemie - Int. Ed.* **2014**, *53* (48), 13020–13041.

https://doi.org/10.1002/anie.201401058.

(21) Rezai, T.; Yu, B.; Millhauser, G. L.; Jacobson, M. P.; Lokey, R. S. Testing the Conformational Hypothesis of Passive Membrane Permeability Using Synthetic Cyclic Peptide Diastereomers. *J. Am. Chem. Soc.* **2006**, *128* (8), 2510–2511. https://doi.org/10.1021/ja0563455.

(22) Chatterjee, J.; Gilon, C.; Hoffman, A.; Kessler, H. N-Methylation of Peptides: A New Perspective in Medicinal Chemistry. *Acc. Chem. Res.* **2008**, *41* (10), 1331–1342. https://doi.org/10.1021/ar8000603.

(23) Doedens, L.; Opperer, F.; Cai, M.; Beck, J. G.; Dedek, M.; Palmer, E.; Hruby, V. J.; Kessler, H. Multiple N -Methylation of MT-II Backbone Amide Bonds Leads to Melanocortin Receptor Subtype HMC1R Selectivity: Pharmacological and Conformational Studies. *J. Am. Chem. Soc.* **2010**, *132* (23), 8115–8128. https://doi.org/10.1021/ja101428m.

(24) Chatterjee, J.; Ovadia, O.; Zahn, G.; Marinelli, L.; Hoffman, A.; Gilon, C.; Kessler, H. Multiple N-Methylation by a Designed Approach Enhances Receptor Selectivity. *J. Med. Chem.* **2007**, *50* (24), 5878–5881. https://doi.org/10.1021/jm701044r.

(25) Biron, E.; Chatterjee, J.; Ovadia, O.; Langenegger, D.; Brueggen, J.; Hoyer, D.; Schmid, H. A. A.; Jelinek, R.; Gilon, C.; Hoffman, A.; Kessler, H. Improving Oral Bioavailability of Peptides by Multiple N-Methylation: Somatostatin Analogues. *Angew. Chemie - Int. Ed.* **2008**, *47* (14), 2595–2599. https://doi.org/10.1002/anie.200705797.

(26) Ter-Avetisyan, G.; Tünnemann, G.; Nowak, D.; Nitschke, M.; Hermann, A.; Drab, M.; Cardoso, M. C. Cell Entry of Arginine-Rich Peptides Is Independent of Endocytosis. *J. Biol. Chem.* **2009**, *284* (6), 3370–3378. https://doi.org/10.1074/jbc.M805550200.

(27) Patel, S. G.; Sayers, E. J.; He, L.; Narayan, R.; Williams, T. L.; Mills, E. M.; Allemann, R. K.; Luk, L. Y. P. P.; Jones, A. T.; Tsai, Y.-H. H. Cell-Penetrating Peptide Sequence and Modification Dependent Uptake and Subcellular Distribution of Green Florescent Protein in Different Cell Lines. *Sci. Rep.* **2019**, *9* (1), 1–9. https://doi.org/10.1038/s41598-019-42456-8.

(28) Wang, C. K.; Northfield, S. E.; Colless, B.; Chaousis, S.; Hamernig, I.; Lohman, R. J.; Nielsen, D. S.; Schroeder, C. I.; Liras, S.; Price, D. A.; Fairlie, D. P.; Craik, D. J. Rational Design and Synthesis of an Orally Bioavailable Peptide Guided by NMR Amide Temperature Coefficients. *Proc. Natl. Acad. Sci. U. S. A.* **2014**, *111* (49), 17504–17509. https://doi.org/10.1073/pnas.1417611111.

(29) Rezai, T.; Bock, J. E.; Zhou, M. V.; Kalyanaraman, C.; Lokey, R. S.; Jacobson, M. P. Conformational Flexibility, Internal Hydrogen Bonding, and Passive Membrane Permeability: Successful in Silico Prediction of the Relative Permeabilities of Cyclic Peptides. *J. Am. Chem. Soc.* **2006**, *128* (43), 14073–14080. https://doi.org/10.1021/ja063076p.

(30) Ghasemy, S.; García-Pindado, J.; Aboutalebi, F.; Dormiani, K.; Teixidó, M.; Malakoutikhah, M. Fine-Tuning the Physicochemical Properties of Peptide-Based Blood–Brain Barrier Shuttles. *Bioorganic Med. Chem.* **2018**, *26* (8), 2099–2106. https://doi.org/10.1016/j.bmc.2018.03.009.

(31) Morimoto, J.; Amano, R.; Ono, T.; Sando, S. A Parallel Permeability Assay of Peptides across Artificial Membranes and Cell Monolayers Using a Fluorogenic Reaction. *Org. Biomol. Chem.* **2019**, *17* (11), 2887–2891. https://doi.org/10.1039/c9ob00133f.

(32) Bárány-Wallje, E.; Keller, S.; Serowy, S.; Geibel, S.; Pohl, P.; Bienert, M.; Dathe, M. A Critical Reassessment of Penetratin Translocation across Lipid Membranes. *Biophys. J.* **2005**, *89* (4), 2513–2521. https://doi.org/10.1529/biophysj.105.067694.

(33) Persson, D.; Thorén, P. E. G.; Esbjörner, E. K.; Goksör, M.; Lincoln, P.; Nordén, B. Vesicle Size-Dependent Translocation of Penetratin Analogs across Lipid Membranes. *Biochim. Biophys. Acta - Biomembr.* **2004**, *1665* (1–2), 142–155. https://doi.org/10.1016/j.bbamem.2004.07.008.

(34) Swiecicki, J. M.; Bartsch, A.; Tailhades, J.; Di Pisa, M.; Heller, B.; Chassaing, G.; Mansuy, C.; Burlina, F.; Lavielle, S. The Efficacies of Cell-Penetrating Peptides in Accumulating in Large Unilamellar Vesicles Depend on Their Ability to Form Inverted Micelles. *ChemBioChem* **2014**, *15* (6), 884–891. https://doi.org/10.1002/cbic.201300742.

(35) Wheaten, S. A.; Ablan, F. D. O.; Spaller, B. L.; Trieu, J. M.; Almeida, P. F. Translocation of Cationic Amphipathic Peptides across the Membranes of Pure Phospholipid Giant Vesicles. *J. Am. Chem. Soc.* **2013**, *135* (44), 16517–16525. https://doi.org/10.1021/ja407451c.

(36) Lein, M.; Deronde, B. M.; Sgolastra, F.; Tew, G. N.; Holden, M. A. Protein Transport across Membranes: Comparison between Lysine and Guanidinium-Rich Carriers. *Biochim. Biophys. Acta - Biomembr.* **2015**, *1848* (11), 2980–2984. https://doi.org/10.1016/j.bbamem.2015.09.004.

(37) Li, X.; Huang, J.; Holden, M. A.; Chen, M. Peptide-Mediated Membrane Transport of

Macromolecular Cargo Driven by Membrane Asymmetry. *Anal. Chem.* **2017**, *89* (22), 12369–12374. https://doi.org/10.1021/acs.analchem.7b03421.

(38) Huang, J.; Lein, M.; Gunderson, C.; Holden, M. A. Direct Quantitation of Peptide-Mediated Protein Transport across a Droplet-Interface Bilayer. *J. Am. Chem. Soc.* **2011**, *133* (40), 15818–15821. https://doi.org/10.1021/ja2046342.

(39) Lee, Y.; Lee, H. R.; Kim, K.; Choi, S. Q. Static and Dynamic Permeability Assay for Hydrophilic Small Molecules Using a Planar Droplet Interface Bilayer. *Anal. Chem.* **2018**, *90* (3), 1660–1667. https://doi.org/10.1021/acs.analchem.7b03004.

(40) Czekalska, M. A.; Kaminski, T. S.; Makuch, K.; Garstecki, P. Passive and Parallel Microfluidic Formation of Droplet Interface Bilayers (DIBs) for Measurement of Leakage of Small Molecules through Artificial Phospholipid Membranes. *Sensors Actuators, B Chem.* **2019**, *286* (September 2018), 258–265. https://doi.org/10.1016/j.snb.2019.01.143.

(41) Faugeras, V.; Duclos, O.; Bazile, D.; Thiam, A. R. Membrane Determinants for the Passive Translocation of Analytes through Droplet Interface Bilayers. *Soft Matter* **2020**, *16* (25), 5970–5980. https://doi.org/10.1039/d0sm00667j.

(42) Strutt, R.; Sheffield, F.; Barlow, N. E.; Flemming, A. J.; Harling, J. D.; Law, R. V.; Brooks, N. J.; Barter, L. M. C.; Ces, O. UV-DIB: Label-Free Permeability Determination Using Droplet Interface Bilayers. *Lab Chip* **2022**, *22* (5), 972–985. https://doi.org/10.1039/D1LC01155C.

(43) Poulin, P.; Bibette, J. Adhesion of Water Droplets in Organic Solvent. *Langmuir* **1998**, *14* (22), 6341–6343. https://doi.org/10.1021/la9801413.

(44) Thiam, A. R.; Bremond, N.; Bibette, J. From Stability to Permeability of Adhesive Emulsion Bilayers. *Langmuir* **2012**, *28* (15), 6291–6298. https://doi.org/10.1021/la3003349.

(45) Ben M'barek, K.; Ajjaji, D.; Chorlay, A.; Vanni, S.; Forêt, L.; Thiam, A. R. ER Membrane Phospholipids and Surface Tension Control Cellular Lipid Droplet Formation. *Dev. Cell* **2017**, *41* (6), 591–604. https://doi.org/10.1016/j.devcel.2017.05.012.

(46) Dougherty, P. G.; Sahni, A.; Pei, D. Understanding Cell Penetration of Cyclic Peptides. *Chem. Rev.* **2019**, *119* (17), 10241–10287. https://doi.org/10.1021/acs.chemrev.9b00008.

(47) Nischan, N.; Herce, H. D.; Natale, F.; Bohlke, N.; Budisa, N.; Cardoso, M. C.;

Hackenberger, C. P. R. Covalent Attachment of Cyclic TAT Peptides to GFP Results in Protein Delivery into Live Cells with Immediate Bioavailability. *Angew. Chemie - Int. Ed.* **2015**, *54* (6), 1950–1953. https://doi.org/10.1002/anie.201410006.

(48) Kwon, Y. U.; Kodadek, T. Quantitative Comparison of the Relative Cell Permeability of Cyclic and Linear Peptides. *Chem. Biol.* **2007**, *14* (6), 671–677. https://doi.org/10.1016/j.chembiol.2007.05.006.

(49) Wang, C. K.; Northfield, S. E.; Swedberg, J. E.; Colless, B.; Chaousis, S.; Price, D. A.; Liras, S.; Craik, D. J. Exploring Experimental and Computational Markers of Cyclic Peptides: Charting Islands of Permeability. *Eur. J. Med. Chem.* **2015**, *97*, 202–213. https://doi.org/10.1016/j.ejmech.2015.04.049.

(50) Buckton, L. K.; McAlpine, S. R. Improving the Cell Permeability of Polar Cyclic Peptides by Replacing Residues with Alkylated Amino Acids, Asparagines, and d -Amino Acids. *Org. Lett.* **2018**, *20* (3), 506–509. https://doi.org/10.1021/acs.orglett.7b03363.

(51) Caillon, L.; Nieto, V.; Gehan, P.; Omrane, M.; Rodriguez, N.; Monticelli, L.; Thiam, A. R. Triacylglycerols Sequester Monotopic Membrane Proteins to Lipid Droplets. *Nat. Commun.* **2020**, *11* (1), 1–12. https://doi.org/10.1038/s41467-020-17585-8.

(52) Campelo, F.; McMahon, H. T.; Kozlov, M. M. The Hydrophobic Insertion Mechanism of Membrane Curvature Generation by Proteins. *Biophys. J.* **2008**, *95* (5), 2325–2339. https://doi.org/10.1529/biophysj.108.133173.

(53) Bird, G. H.; Mazzola, E.; Opoku-Nsiah, K.; Lammert, M. A.; Godes, M.; Neuberg, D. S.; Walensky, L. D. Biophysical Determinants for Cellular Uptake of Hydrocarbon-Stapled Peptide Helices. *Physiol. Behav.* **2017**, *176* (1), 139–148. https://doi.org/10.1038/nchembio.2153.Biophysical.

(54) Gehan, P.; Kulifaj, S.; Soule, P.; Bodin, J. B.; Amoura, M.; Walrant, A.; Sagan, S.; Thiam, A. R.; Ngo, K.; Vivier, V.; Cribier, S.; Rodriguez, N. Penetratin Translocation Mechanism through Asymmetric Droplet Interface Bilayers. *Biochim. Biophys. Acta - Biomembr.* **2020**, *1862* (11), 183415. https://doi.org/10.1016/j.bbamem.2020.183415.

(55) Nigsch, F.; Klaffke, W.; Miret, S. In Vitro Models for Processes Involved in Intestinal Absorption. *Expert Opin. Drug Metab. Toxicol.* **2007**, *3* (4), 545–556. https://doi.org/10.1517/17425255.3.4.545.

(56) Hallifax, D.; Turlizzi, E.; Zanelli, U.; Houston, J. B. Clearance-Dependent Underprediction of in Vivo Intrinsic Clearance from Human Hepatocytes: Comparison

with Permeabilities from Artificial Membrane (PAMPA) Assay, in Silico and Caco-2 Assay, for 65 Drugs. *Eur. J. Pharm. Sci.* **2012**, *45* (5), 570–574. https://doi.org/10.1016/j.ejps.2011.12.010.